Imperfection sensitivity of externally pressurised shells

Static and pulse loading

Jan Blachut

The University of Liverpool
Department of Engineering
Liverpool L69 3GH, UK
em20@liverpool.ac.uk

ABSTRACT. *The paper examines the sensitivity of buckling loads to the initial geometric imperfections in metallic cylindrical, toroidal, barrelled and torispherical shells subjected to uniform external pressure. The adopted approach is based on the FE analysis of a number of selected cases. The imperfection profiles include either localised (stripe, cos x cos, increased-radius flattening, etc.) or global (modulated eigenmode) distortion of shell's mid-surface. The lower bound methodology has been adopted for all localised shape deviations. Differences between buckling sensitivities to localised and global imperfections are given for the following cases: (i) for cylinders subjected to radial pressure, (ii) for toroids and torispheres subjected to static external pressure. It is shown here that the largest reduction of the buckling strength is not associated with one particular form of shape deviations. In bowed out shells the eigen-imperfections seem to be affecting the load carrying capacity to a lesser extent than in equivalent cylinders. Dynamic failure loads of imperfect torispheres are smaller than their static ones but only for up to threshold magnitudes.References to previous buckling experiments on perfect and imperfect shell components are also provided.*

KEYWORDS: *Buckling, External pressure, Shape imperfections.*

Revue européenne des éléments finis. Volume 13 – n° 8/2004, pages 787 to 810

1. Introduction

This paper complements the previous studies on the load bearing capacity of externally pressurised shells which contain initial geometric imperfections (Blachut and Jaiswal 1999a, b 2000). Several shell geometries are considered in the paper and this includes cylinders, barreled shells with positive Gaussian curvature, closed toroids and domed end-closures. It is assumed that these shell components are to be used in pressure vessels subjected to either external pressure or to a vacuum condition. This is a numerical study in which calculations were carried out for static and for suddenly applied pressures. The latter had either ramp or step time profile. The primary mode of failure of the above mentioned shells, when they are geometrically perfect, is either through bifurcation buckling, axisymmetric snap-through (under static load) or through the uncontrolled growth of steady state amplitude (under pulse load).

The existence of the initial geometric imperfections can adversely affect the load carrying capacity of considered shells with the detrimental factors being imperfections' shape, its positioning, size and depth. There are also other factors which can affect the buckling performance of shell components, and these include, for example, loading imperfections, imperfect boundary conditions, inhomogenous material, residual stresses, etc. References (Cederbaum and Arbocz 1996, Godoy 1996, Kinght and Starnes 1997, Godoy and Taraco 2000), for example, address these important aspects of shells' load bearing capacity in details, whilst this paper examines only the initial shape deviations from perfect geometry and their effect on buckling/collapse. Geometric imperfections can take various forms and several of them, of global and local nature, are explored in the paper. The global imperfections include shape deviations in the form of the eigenmode associated with the asymmetric bifurcation buckling. Apart from global shape distortion, *i.e.*, with the affinity to eigenmodes, one can experience a wide range of localised shape deviations from the perfect geometry. A local indentation or flattening of the shell's surface are the most frequently studied profiles. In this paper an inward dimple was modelled in the following three ways: (i) using a polynomial patch with a smooth blending into the remaining portion of perfect geometry, (ii) using a cosine function in two directions with the cusp-type edge between the patch and geometrically perfect portion of the shell, and (iii) using cosine function in two directions with a smooth blending into the perfect geometry. The lower bounds of the load carrying capacity were then evaluated numerically and compared. For some shells the eigenmode can have a large number of circumferential waves. Since such waviness of shell surface would normally be unrealistic in practice, it was decided to examine an imperfection profile confined to 'a single wave' dimple extracted from the eigenmode.

In the case of static pressure, the elastic and elastic-plastic buckling analyses were carried out for geometrically imperfect cylinders, toroids, bowed out shells and domes. Elastic buckling caused by the pulse loading was studied for domes, only.

Results given in the paper are based on Abaqus, Bosor5 and LS Dyna codes, (Hibbitt *et al*., 1998, Bushnell, 1976, Hallquist, 1997). The paper provides references to experimental results on CNC-machined, mild steel barrels, on spun steel toroids, and on injection moulded torispheres (*i.e*. experimental results which were obtained in Liverpool). The latter shells had built-in local flat patches into their geometry.

The main motivation behind this study is to illustrate to what extend the buckling strength can be affected by various imperfection profiles.

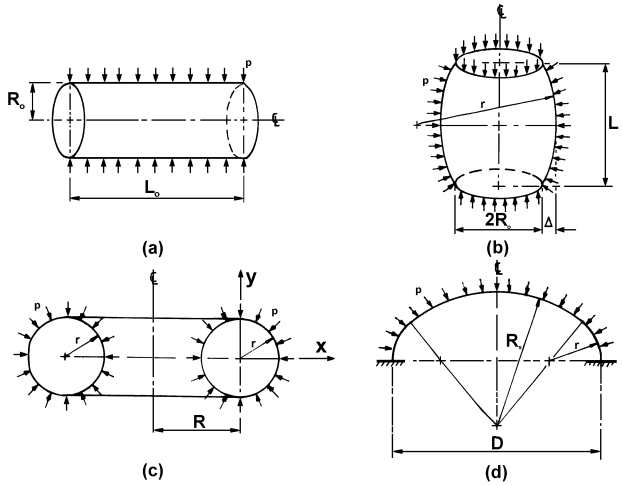

Figure 1. *Shell geometries considered in the paper (cylindrical, bowed out, toroidal and torispherical)*

2. Modelling details

Four geometries which are discussed in this paper are sketched in Figure 1. The cylinder, sketched in Figure 1a, is subjected to the radial pressure, only. Fully clamped boundary conditions are applied at both ends. The bowed out shell is subjected to external hydrostatic pressure and its ends are allowed to move axially whilst all other deflections and rotations are set to zero at the ends. The meridional profile of the barrel is to be modelled by a circular arc - as specified later. The closed toroid, shown in Figure 1c, will be restrained at the inner and outer equators, only. References will be made later to previous results where the effect of boundary conditions on the load carrying capacity has been assessed. The cross-section may not necessarily be circular and results for toroids with elliptical cross-sections are also to be discussed. Torispherical end closures, sketched in Figure 1d, are clamped at the base perimeter and there is no cylindrical flange attached to the knuckle. The wall thickness is assumed constant for all considered geometries (whether geometrically perfect or imperfect).

3. Cylindrical shells

The background to static stability of cylindrical shells subjected to uniform external pressure can be found, for example, in (Samuelson and Eggwertz, 1992, Nash, 1995, Guggenberger, 1995, Ross, 2001). The reference by Guggenberger, 1995, discusses static buckling behaviour of geometrically imperfect cylinders subject to vacuum. It provides numerical and experimental results for cylinders with a single longitudinal dent. Two imperfection profiles of stripe-type, are modelled and comparison with experimental data on four, 400 mm long shells, is given. The length-to-radius ratio of considered shells was 2.0 and the radius-to-thickness ratio was 200. The major finding reported in the paper implies that relatively narrow longitudinal and inward stripe-dimple is not greatly affecting the buckling load's magnitude. The drop of up to 11% below the buckling pressure of a geometrically perfect model was recorded numerically and this magnitude was confirmed experimentally. The other conclusion was that the actual shape of the inward dent did not play any significant role in lowering the load carrying capacity of considered shells. The narrow axial patches, studied by Guggenberger, 1995, are to be extended in this paper, to localised patches with variable hoop and axial lengths. References (Schneider, 1996, Teng and Song, 2001, Brede and Schneider, 2003) provide detailed information about experimental/numerical results into buckling of geometrically imperfect cylinders. Good comparison between test results obtained for carefully manufactured imperfect cylinders, and numerical predictions of the corresponding buckling loads, is reported by Schneider 1996. Both, Schneider 1996 and Teng and Song 2001, consider shape deviations which are related to eigenshapes.

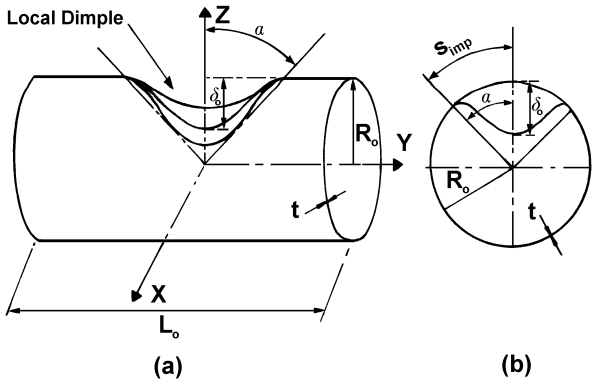

Figure 2. *Geometry of a localised, inward dimple in a cylindrical shell. The imperfect patch covers the area cut-out by a cone with its tip at the origin of (XYZ) co-ordinate system*

3.1. *Elliptical dimple*

As a first example, let us consider a localised dimple positioned at the middle of the cylinder's axial length, L_o - as sketched in Figure 2. The imperfect area covers the surface which is cut-out from cylinder by a cone with the semi-angle, α. The imperfection length measured over the cylinder's surface is $s_{imp1} = \alpha R_o$ in the hoop direction and it is $s_{imp2} = R_o \tan\alpha$ along the Y-axis of the cylinder.

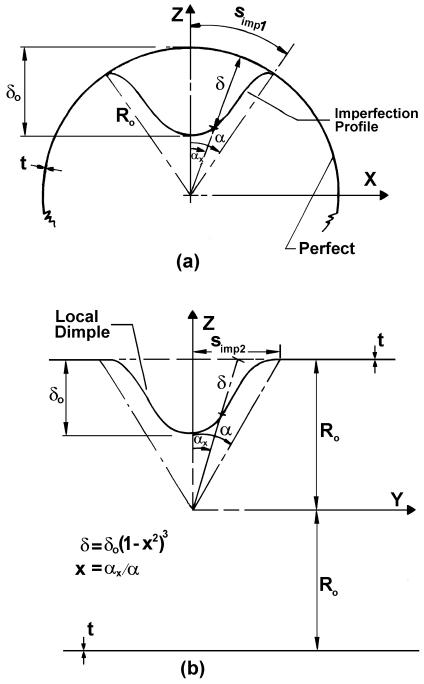

Figure 3. *Modelling details for the smooth, inward dimple. Views along the Y-axis (Figure 3a) and perpendicular to the cylinder (Figure 3b)*

The maximum amplitude of inward indentation is, δ_o, and the radial deviation, δ, from the perfect shape is assumed as follows:

$$\delta = \delta_o (1-x^2)^3, \qquad \text{where } x \equiv \alpha_x/\alpha. \qquad [1]$$

This modelling is shown in Figure 3. Let us note here that the imperfection patch blends smoothly into the cylindrical shell along an elliptical edge.

Numerical calculations have been carried out for cylindrical shell in which the length-to-radius ratio is, $L_o/R_o = 4$, the radius-to-thickness ratio is, $R_o/t = 100$ and the yield point of material is, σ_{yp} = 300 MPa. This cylinder looses its load carrying

capacity, when perfect, by bifurcation buckling with n = 5 circumferential waves. The magnitude of the buckling pressure is p_{bif} = 0.690 MPa (from Bosor5) and p_{bif} = 0.687 MPa (from Abaqus). The subsequent calculations have been carried out using the Abaqus FE code. The first set of results corresponds to the fixed extent of the local imperfection patch determined by $\alpha = 25^o$. The structural response has been measured for dimensionless amplitude of the imperfection, δ_o/t, varying between 0.0 and 1.0. The obtained results are shown in Figure 4 where it is seen that all imperfect geometries lost the load carrying capacity through the collapse mechanism at marginally smaller magnitude than the bifurcation buckling pressure of a perfect cylinder. Results corresponding to the lower-bound approach are also depicted in Figure 4. For a given amplitude of the imperfection, the angle, α, has been varied and the lowest failure pressure has been recorded. It is seen that this type of initial shape deviation from perfect geometry leads to about 10% reduction of the load carrying capacity (for δ_o/t = 1.0). The above two curves are compared in Figure 4 with the response obtained for the imperfection shape taken in the form of the eigenmode. In this case the reduction of the load carrying capacity is much greater and it is about 45% below the magnitude of buckling pressure of a perfect shell (again for δ_o/t = 1.0). Magnified views of shape deviations, corresponding to δ_o/t = 0.75, are also shown in Figure 4.

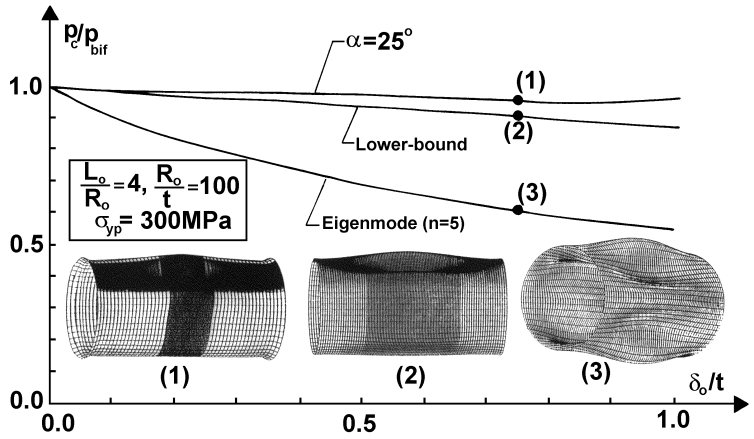

Figure 4. *Sensitivity of buckling pressure to different deviations from perfect geometry. Magnified imperfect configurations, for δ_o/t = 0.75, are also shown. Note that cases (1) and (2) correspond to local imperfection and the case (3) corresponds to modulated eigenmode imperfection*

The above results were obtained for a single value of the yield point of material, *i.e.*, for σ_{yp} = 300 MPa. Further two sets of results were obtained for elastic material and for the yield point of material σ_{yp} = 200 MPa. Results are depicted in Figure 5. The inclusion of plasticity makes the load carrying capacity of the cylindrical shell

more sensitive to initial geometric imperfections which have an affinity to eigenmodes.

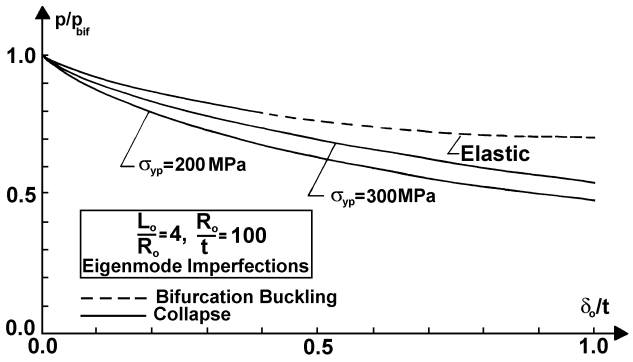

Figure 5. *The effect of the yielding point of material on the imperfection sensitivity (for a cylindrical shell)*

3.2. *Rectangular dimples*

If the imperfection has a significantly different length in the hoop than in the axial directions then the following two parametrisations can be useful. The first one forms an indentation of 'a cusp-type edge' with the perfect geometry. Shape of the imperfect patch is described as follows:

$$\Delta\bar{z} = \delta_o \cos(\pi\bar{x} / 2a)\cos(\pi\bar{y} / 2b)\,. \qquad [2]$$

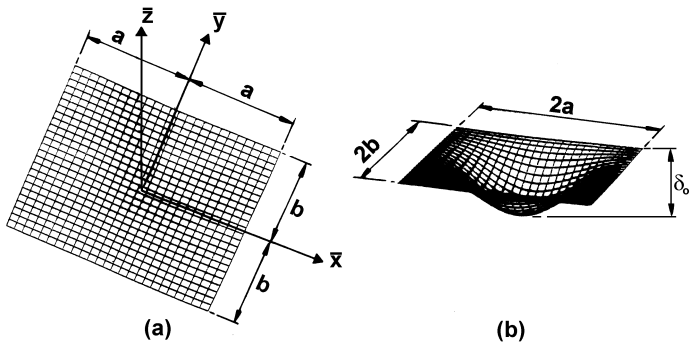

Figure 6. *View of flat grid 2a x 2b (Figure 6a) being converted into a cos x cos dimple (Figure 6b)*

Figure 6 depicts a rectangular (2a x 2b) patch and the corresponding (cosine x cosine) inward dimple with the amplitude, δ_o. The second, smooth patch along the edge, is given by the following equation:

$$\Delta\bar{z} = 0.25\delta_o[1+\cos(\pi\bar{x}/a)][1+\cos(\pi\bar{y}/b)] \qquad [3]$$

Equations [3] and [4] allow to model inward indentations of narrow longitudinal stripe-type shape, as well as, a narrow patch running in hoop direction - as sketched in Figures 7b, 7d (for the dimple's profile given by Equation [3]). Figure 7 also shows two other possible initial geometric imperfections, *i.e.*, smooth elliptic dimple, Figure 7a, and an eigenvector-type global imperfection, Figure 7c.

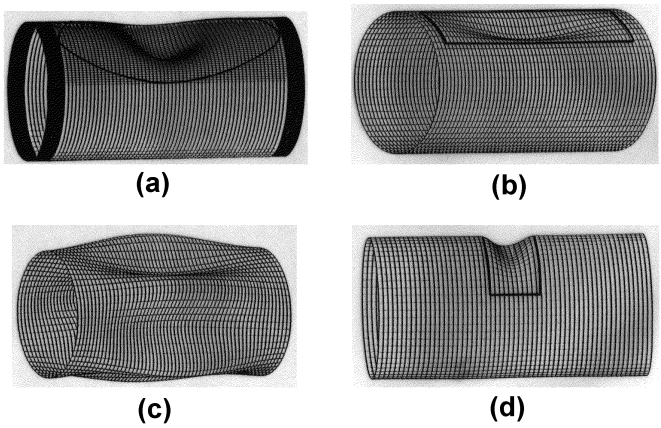

Figure 7. *View of three localised dimples and the eigenshape-type initial deviation from perfect geometry in a cylinder*

Comparison is made in Figure 8 of the influence of these four forms of shape deviations from perfect geometry on the load carrying capacity of a cylinder. It is seen here that all inward dimple-type imperfections reduce the buckling pressures much less than the eigenshape-type imperfection. The results for local, dimple-type imperfections, are the lower-bound results. For (cosine x cosine) patches they were obtained by investigating the grid $0 \le 2b \le L$ and $0 \le 2a \le 0.1\pi R_o$.

Results of the above calculations suggest that the buckling strength is not greatly affected by various forms of local dimples. By far the worst shape imperfection appears to be the eigenmode profile. When the magnitude of hoop waviness is changed then the sensitivity of buckling load diminishes. This is illustrated in Figure 9 for the wave numbers n = 6, 7 and 10 as opposed to the eigenmode $n \equiv 5$. It is seen here that for the larger wave number, *e.g.*, for n = 10, the sensitivity approaches the one which has been obtained for the lower bound approach (see Figure 8).

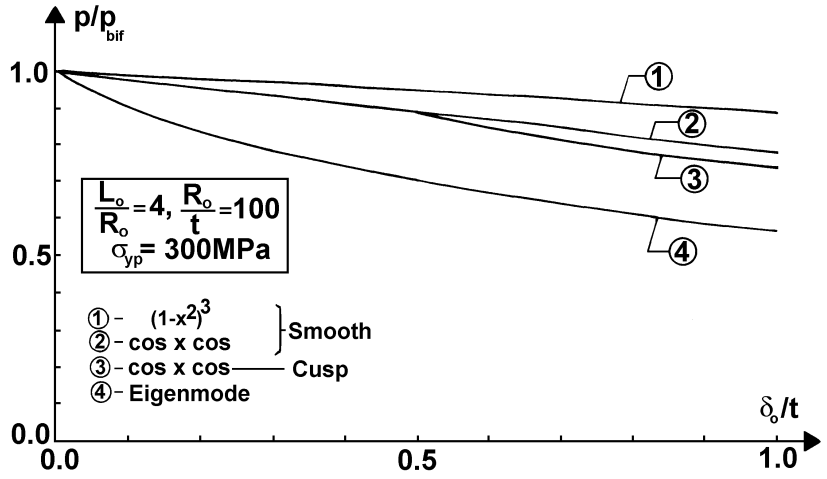

Figure 8. *Relative imperfection sensitivity of buckling loads to four types of initial geometric shape imperfections*

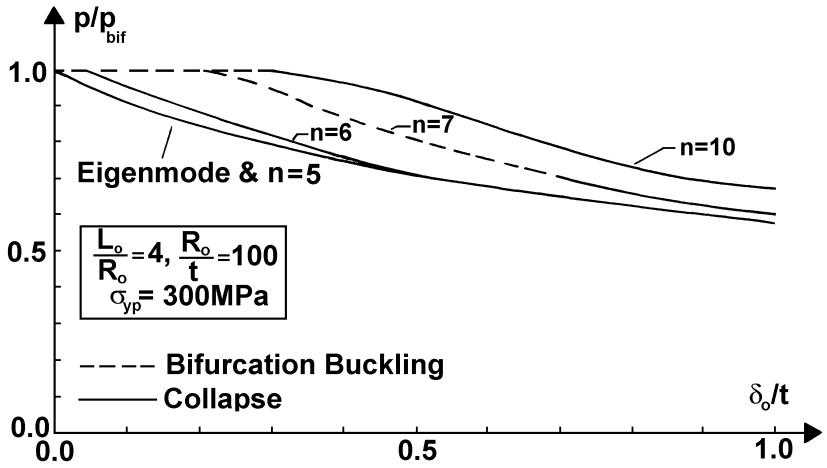

Figure 9. *Influence of different imperfection shape on the buckling load in a cylinder*

4. Bowed out shells

Let us consider a bowed-out shell of length, L, and with its meridian being described by a circular arc - as sketched in Figure 1b. Buckling performance of a barrel can be assessed on a like-for-like basis if one assumes, for example, that the mass of a cylindrical shell and that of a barrel are the same. Let us also assume that

the radii at the top and bottom edges of a barrel are the same and they equal to the radius of a cylindrical shell, R_o.

The amount of barrelling, Δ, can then be found from the condition of constant mass - see Blachut and Wang 2001 for further details.

Typical curves depicting buckling pressure versus the amount of barrelling, Δ, are given in Figure 10 for four sets of boundary conditions at the top and bottom edges of the barrel. In all four cases the axial displacement, at the top and bottom edges, is not constrained and the edges can move freely. The upper two curves correspond to the radial displacement, w, being set to zero. The lower two curves correspond to the variable, w, being free. It is seen from Figure 10 that significant pressure increase can be obtained by bowing out a cylindrical shell. For $L_o/R_o = 2.0$, $R_o/t = 33.3$ and the yield point of material, $\sigma_{yp} = 300$ MPa, the maximum pressure which the bowed out shell can support is p = 14.60 MPa (see point 'a' in Figure 10). This represents the increase of 44% above the bifurcation buckling pressure of the mass equivalent cylindrical shell. It appears that there have been no attempts to assess the imperfection sensitivity of bowed out shells which are subjected to static external pressure. It is obvious from Figure 10 that the failure mode at the optimum is the axisymmetric collapse.

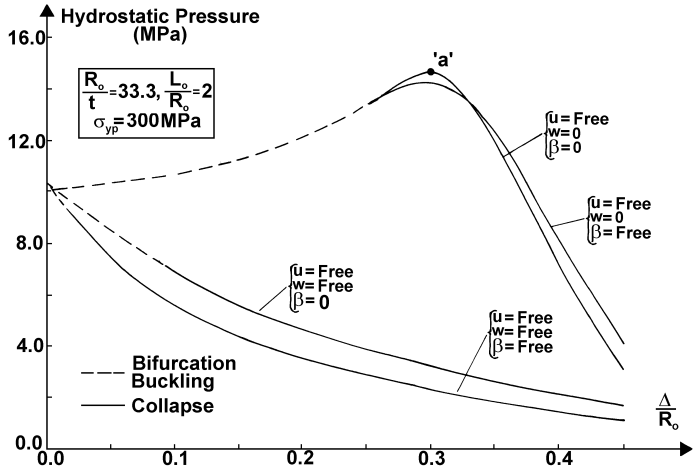

Figure 10. *The effect of barrelling on the buckling load for four sets of boundary conditions at the top and bottom edges. Note that the largest increase of buckling load has been obtained when no rotation, β, nor radial displacement, w, are allowed at the ends*

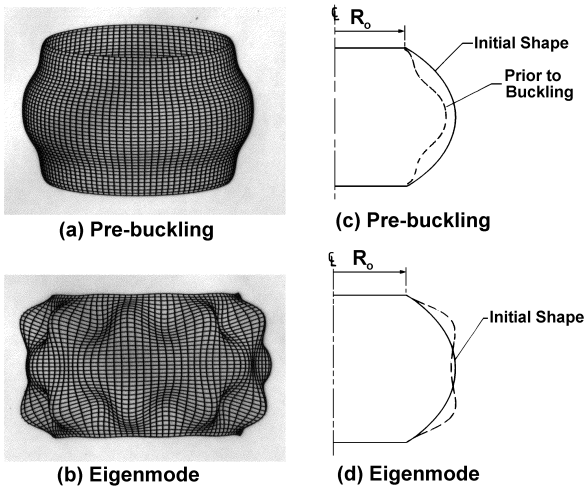

Figure 11. *Pre-buckling and buckling shapes of bowed out shell for elastic material properties. The shell's geometry corresponds to optimal geometry (point 'a' in Figure 10)*

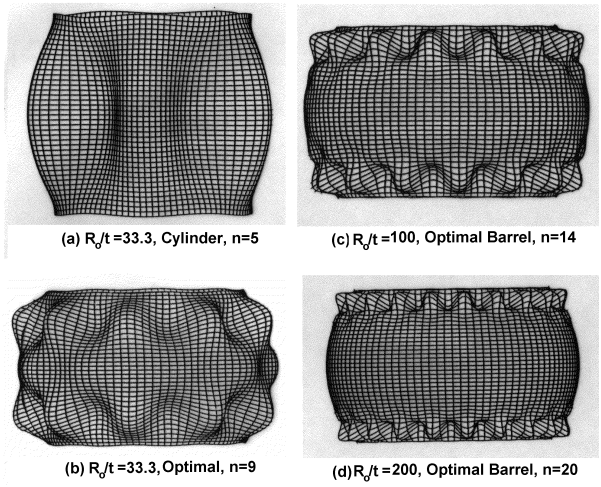

Figure 12. *Eigenshape of mass equivalent cylinder (Figure 12a). Elastic eigenshapes of optimal geometry for three different wall thicknesses (R_o/t_o = 33.3, 100 and 200)*

One way of generating a test imperfection shape is to assume its elastic eigenmode. Figure 11 shows the prebuckling and buckling shapes as well as the corresponding sections through the barrel corresponding to point 'a' in Figure 10

under the assumption of elastic buckling. Other eigenmodes, for the same meridional profile, are depicted in Figure 12 for various R_o/t ratios, *i.e.*, for R_o/t = 33.3, 100 and 200. It is seen here that the waviness of the eigenshape occurs simultaneously close to the top and bottom edges. Results in Figure 13 show how the load carrying capacity of the optimal barrel can be affected when the above eigenshapes are used as the initial shape deviations from perfect geometry. The same figure compares the sensitivity of buckling load to eigenshape imperfections in the mass equivalent cylindrical shell. It is seen here that the buckling pressure for the cylindrical geometry is more sensitive to imperfections than in bowed out shell of the same mass. This appears to contradict the usual trend where 'optimal configurations' tend to be 'less robust' when subjected to deviations from perfect solution.

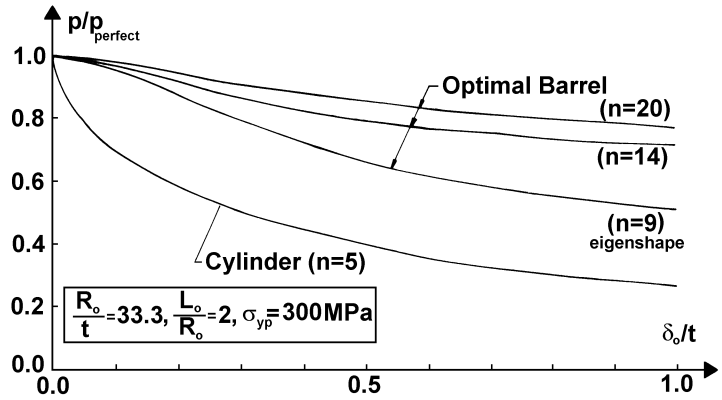

Figure 13. *Comparison of imperfection sensitivity obtained for cylinder and for three barrels*

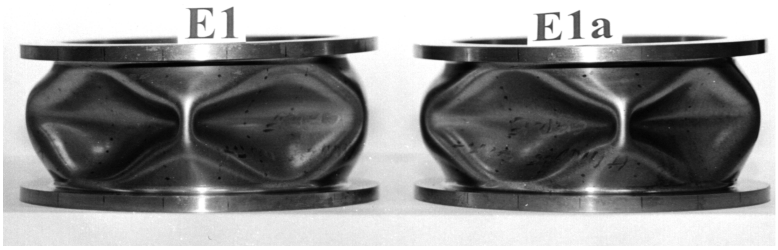

Figure 14. *View of two, nominally identical mild steel barrels, after the collapse (from Blachut 2003, $p_{coll} \cong 17$ MPa)*

Experimental results on eight CNC-machined, mild steel shells are provided in Blachut 2001, 2002 and 2003. All models were collapsed by static external pressure

and Figure 14 depicts two, nominally identical barrels, after the test. These were 'near-perfect' models and it remains difficult to conclude whether buckling loads in barrels are less sensitive to standard imperfection profiles than in equivalent cylinders. This aspect of the problem requires further investigations.

5. Toroidal shells

Recently, there has been a renewed interest in buckling performance of closed toroidal shells due to vacuum and underwater applications. Review of the past theoretical and experimental work into buckling of complete toroidal shells can be found in Galletly and Blachut, 1995. Two strands of carried out work have concentrated on the effect of boundary conditions on the buckling strength and on the effect of the cross-section shape on the magnitude of buckling pressure – Galletly and Blachut, 1995, Blachut and Jaiswal, 1999, 2000. In what follows, a brief account is given of the imperfection sensitivity under static pressure loading for complete toroidal shells with elliptical and circular cross-sections. It is assumed that different pre-buckling and buckling boundary conditions are applied along the inner and outer equators. Out of many combinations for Boundary Conditions, BCs, only the configuration leading to the lowest bifurcation buckling is adopted here. The following BCs are assumed during the pre-buckling analysis: $\{u_x \neq 0, u_y = u_z = \Phi_x = \Phi_y = \Phi_z = 0\}$ and these restraints are applied simultaneously at both the inner and outer equators. The buckling BCs are taken as: $\{u_x \neq 0, u_y = u_z = \Phi_x = 0, \Phi_y \neq 0, \Phi_z = 0\}$ and they are applied along perimeter of the inner equator, only. The outer equator is left unconstrained during the buckling phase of the analysis.

Let us consider a complete and geometrically perfect toroidal shell with a circular cross-section, as sketched in Figure 1c. An interesting buckling performance can be obtained for toroids with an elliptical rather than circular cross-section (Figure 15b). For prolate cross-sections, *i.e.*, for cross-sections having a > b in Figure 15b, one can obtain buckling pressures which are several times higher than the buckling pressures for the equivalent circular cross-sections. Figure 16 depicts typical results for a mild steel toroid described by R/r = 4.0, r/t = 100 and under the assumption that the material remains either elastic or elastic perfectly-plastic. Elastic analyses show that for toroids with a/b < 1 the buckling pressures are smaller than buckling pressures for the equivalent circular cross-section toroids (a≡b=r). For 1.0 < a/b < 1.91 the buckling mode corresponds to n = 0 and the eigenvalue continuously increases between a/b = 1.0 and a/b ≅ 1.91. For a/b > 1.91 there is a sudden change of the eigenshape from n = 0 to n > 0. Also, the magnitude of buckling pressures begins to decrease. It is of interest now to examine the behaviour of non-circular toroids once they are geometrically imperfect. Two imperfection profiles have been studied for the above toroidal geometry. One of them is based on the eigenshape imperfection and typical results are depicted in Figure 16. It is seen that the mode, n = 0, leads to less sensitive response than the mode n > 0. The differences in the magnitude of load carrying capacity are significant and this remains true for both the elastic and elastic-plastic modelling of the material. Results shown in Figure 16 suggest that from a

design point of view it would be advantageous to choose an elliptical cross-section with a/b < 1.91 in order avoid the high sensitivity for eigen-profiles appearing in geometries with a/b > 1.91.

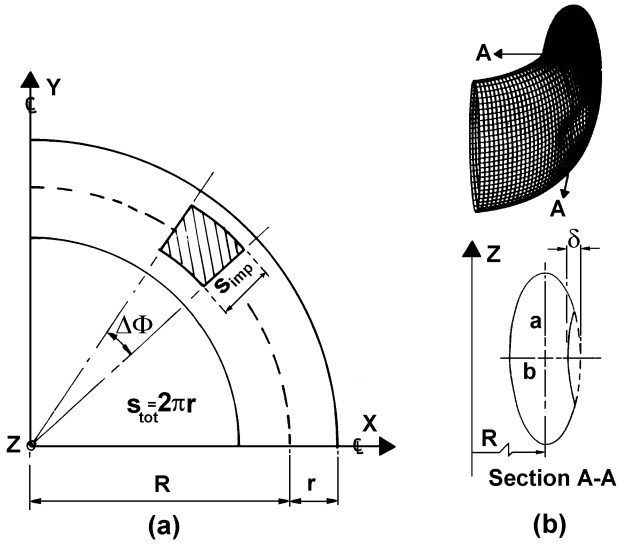

Figure 15. *Planar view of flat patch (Figure 15a). View of a rectangular dimple positioned at the outer equator in a toroid with an elliptical cross-section*

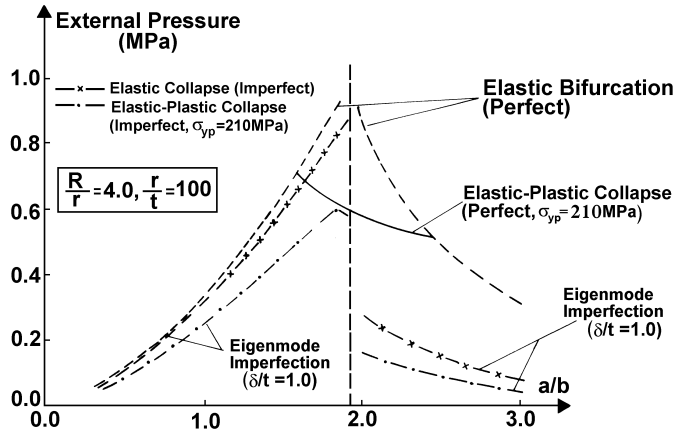

Figure 16. *Plot of buckling pressure versus the semi-axes a/b - ratio in a complete toroid. The effect of eigenmode imperfection on the load carrying capacity is shown for both elastic and elastic-plastic modelling of mild steel*

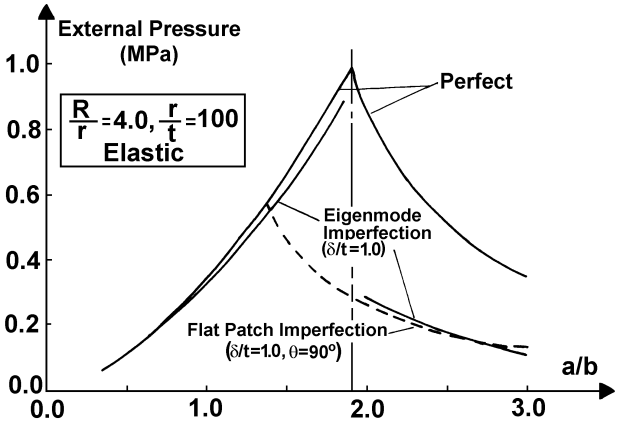

Figure 17. *Comparison of imperfection sensitivities obtained for two models of shape deviations from perfect geometry,* i.e.*, for eigenmode and for local dimple profiles across the range of (a/b)-ratios*

A local dimple given by Equation [2] was the second imperfection profile which has been analysed here. Its planar view is shown in Figure 15a, whilst a magnified view is depicted in Figure 15b for the dimple's position at the outer equator, *i.e.*, for $\theta = 90^o$.

Results, displayed in Figure 17, show that this kind of dimple leads to more-or-less the same sensitivity as for the eigenmode imperfections (for a/b > 1.91). At the same time, this imperfection profile drastically reduces the load carrying capacity, to the level well below that which had been obtained for the eigenmode, n = 0, imperfections (for a/b < 1.91). This detrimental effect of the localised dimple is strongly dependent on the a/b - ratio, *i.e.*, on the cross-section profile of the toroid. The results shown in Figure 17 correspond to the dimple being positioned at the outer equator. Further calculations have been carried out in order to assess the influence of other r-hoop positions as well. A single and arbitrarily chosen semi-axis ratio, a/b, was assumed in these calculations, *i.e.*, a/b = 2.6. The appropriate results are provided in Table 1. It is clear that the dimple's position at, $\theta = 90^o$, corresponding to the outer equator location, is the most detrimental position. Details of further parametric studies can be found in (Blachut and Jaiswal, 2000).

It has to be said that very little experimental data exists to support theoretical results on buckling of externally pressurised toroids (whether perfect or imperfect - see Blachut 2003, for example).

Table 1. *Sensitivity of buckling pressures to the position of the local, inward, dimple around the r-circumference in toroidal shell ($\theta = 0^o \equiv$ north pole; $\theta = 90^o \equiv$ outer equator, etc.). Results are based on the lower-bound approach, $\delta_o/t = 1.0$ and elastic modelling of the material. The perfect geometry is given by R/r = 4.0, r/t = 100 and a/b = 2.6. Note: c ≡ collapse; n = 35 corresponds to 35 circumferential waves at the bifurcation mode*

Dimple's position [θ^o]	External Pressure [MPa]
0	0.465(35)
30	0.43(c)
39	0.38(c)
45	0.21(c)
60	0.172(c)
90	0.159(c)
105	0.166(c)
120	0.194(c)
135	0.227(c)
150	0.43(c)
180	0.465(35)
210	0.465(35)
270	0.465(35)

6. Torispherical domes

The background information on buckling of externally pressurised metallic torispherical pressure vessel end closures, including the current design philosophy, can be found, for example, in (Samuelson and Eggwertz, 1992 ; Nash, 1995 ; Ross, 2001 and in Lu *et al*., 1995 ; Blachut, 1998 ; Albertin, 2000 ; Wunderlich and Albertin 2002). It is known that domes' design against buckling caused by static external pressure is based on the knock-down factor approach. This philosophy stems from high sensitivity of buckling loads to initial geometric imperfections. Typical numerical results obtained for metallic domes, with some of the outstanding issues being discussed, is provided next.

6.1. *Static loading*

Let us consider a torispherical dome sketched in Figure 1d. Most of the past research effort has concentrated on assessing the effect of geometrical imperfection positioned in the spherical portion. Various imperfection profiles had been adopted

in numerical studies which have then been carried out. Local dimples were usually placed at the apex and, in a sense, they provided information on sensitivities for the spherical part of a dome. The eigenmode usually spans the edge between the spherical cap and the knuckle and there have been doubts whether the obtained sensitivities are relevant for torispheres with a generous knuckle. Blachut and Jaiswal, 1999, have examined a local dimple which had been moved from the spherical portion, through the spherical cap/knuckle junction and into the knuckle itself. Numerical results showed that indeed shape deviations at a junction lead to a larger reduction of the buckling strength than a similar imperfections in the spherical part, away from the cap/knuckle junction.

Previous work has also shown that the eigenshape imperfections may not lead to the largest reduction of the load carrying capacity, (Blachut and Jaiswal 1999). This is demonstrated in Figure 18 for a torispherical head with $R_s/D = 1.0$, $r/D = 0.2$ and $D/t = 500$. As expected, the eigenshape-type, global imperfection drastically reduces the buckling strength for small amplitudes of imperfections but for larger amplitudes it appears that the trend is reversed. Similar results can be found in (Galletly and Blachut 1995). Equally important point is the waviness of the eigenmode and how relevant is the waviness from a practical point of view? Results shown in Figure 18 suggest that there is not much difference between the sensitivity to the full eigenmode shape of the imperfection and to a single wave imperfection extracted from that eigenmode.

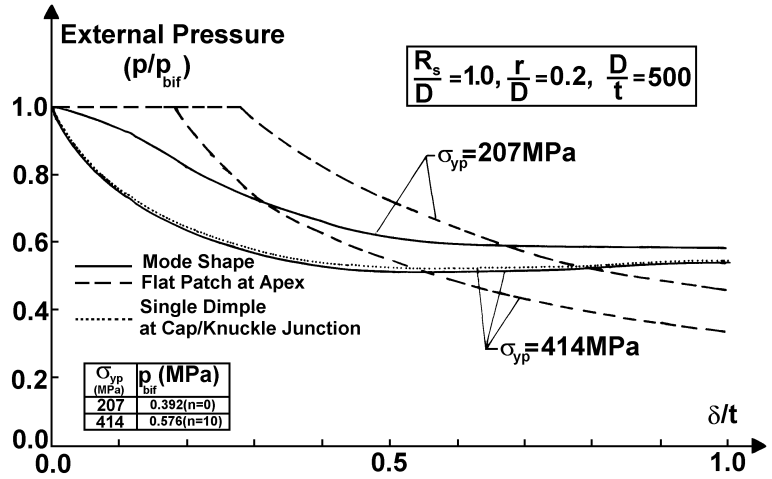

Figure 18. *Sensitivity of buckling load in externally pressurised torisphere. Comparisons are shown for eigenmode, single wave extracted from the eigenmode and increased-radius flat patch positioned at the apex (lower-bound calculations). The yield points of mild steel are, σ_{yp} = 207 MPa and 414 MPa*

The local dimple imperfection, on the other hand, shows that a torisphere can sustain small amplitude local shape deviations without any consequence and only after a threshold value of the imperfection amplitude is exceeded, then buckling load's magnitude starts to be affected, *i.e.*, it decreases - as shown in Figure 19. This observation has been a subject of experimental validation and Figure 19 summarises the obtained results. As a result of lower-bound-calculations, four imperfect configurations have been identified for experimentation. Five steel moulding tools were used in total (one for perfect geometry, plus further four for torispheres with increased-radius flattened patches). The corresponding torispheres have been moulded from the ABS plastic and they were tested under the vacuum conditions. Hundred fifty shells were tested (30 per given geometry). All shells failed suddenly into a multi-lobe shape (for perfect geometry, and for $\delta_o/t = 0.05$), or into a single lobe positioned at the imperfection patch (for all other geometries). The experimental results have confirmed the FE-predictions - as shown in Figure 19 (see Blachut and Jaiswal 1999; Blachut 1998; for further details).

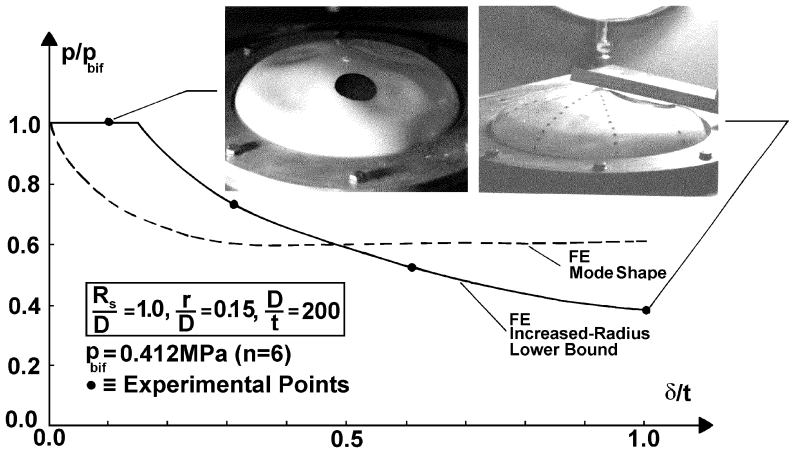

Figure 19. *Comparison of FE predictions with experimental results for geometrically imperfect torisphere (increased-radius flat patch positioned at 12^o away from the apex - see the black patch at the inserts). Also, sensitivity of elastic buckling to the eigenmode-type imperfection*

6.2. *Pulse loading*

Let us now consider a step and ramp external pressure profiles of infinite duration applied to an elastic torisphere sketched in Figure 1d. The dynamic response of the elastic torisphere under step and ramp profiles of external pressure was recorded using the LS-Dyna code. Two types of initial geometric imperfections were introduced into the dome, *i.e.*, increased-radius flat patch positioned at the apex and eigenmode type imperfection.

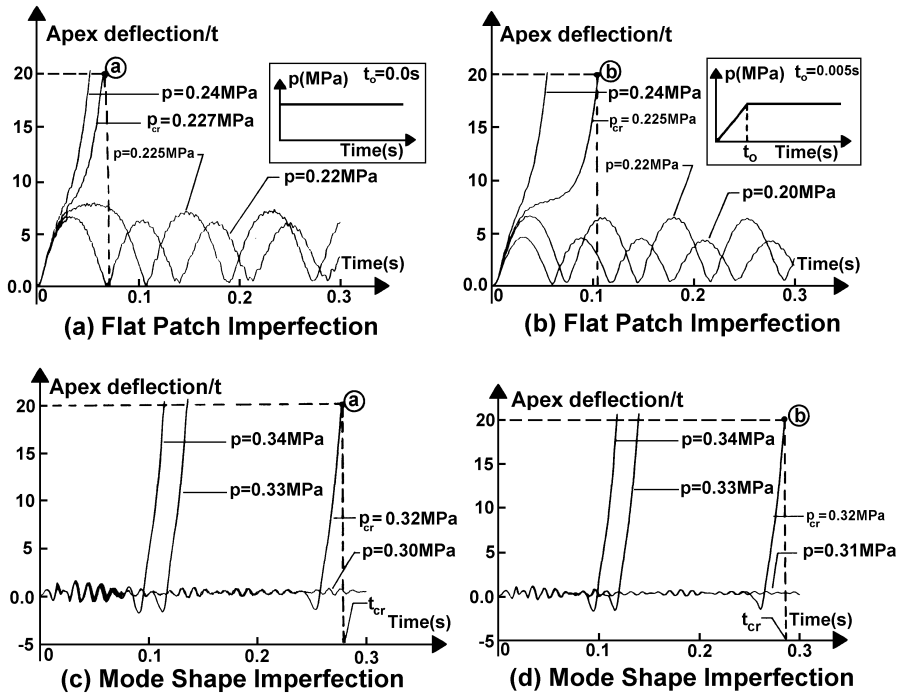

Figure 20. *Response time histories of apex deflection of an imperfect torisphere with δ_o/t = 1.0 (R_s/D = 1.0, r/D = 0.2, D/t = 500). The step pressure has been applied to cases depicted in Figures. 20a and 20c. The ramp pressure profile, with t_o = 0.005, corresponds to Figures. 20b and 20d*

Typical time histories of apex deflections due to step and ramp loading are shown in Figure 20 for an imperfect dome (with flat patch and eigenmode imperfection profiles). After the application of the load there are two possibilities.

In the first one, the shell can vibrate for a number of cycles and then there is a sudden increase in the amplitude indicating an indirect snapping - see a trace corresponding to p = 0.32 MPa in Figure 20d, for example. To quantify the time to snapping it was decided to define the time corresponding to (apex deflection/t) = 20 as the critical time, t_{cr}. The lowest value of pressure, p, at which the shell fails, *i.e.*, it snaps is called the critical pressure, p_{cr}. In Figure 20d the critical pressure is, p_{cr} = 0.32 MPa and the corresponding critical time is, t_{cr} = 0.285s.

The second type of response, known as direct snapping, is illustrated in Figures 20a and 20b. They show the dynamic response for a dome with flat patch. It is seen here that snapping occurs very quickly, and this mode of failure is called a direct snapping.

Variation of the critical time which was obtained for step and ramp profiles of external pressure is depicted in Figure 21. These results were obtained for the imperfection amplitude, δ/t = 0.3, 0.5 and 1.0. It is seen here that the critical time becomes larger for smaller values of snapping pressures. It is also seen that below a certain threshold value of pressure the snapping mechanism does not occur even for a very large value of time. Direct comparison of static and dynamic loadings' sensitivities to imperfections in torispheres, suggests that for 'smaller' magnitudes of imperfections the dynamic buckling loads are more sensitive than the static buckling pressures.

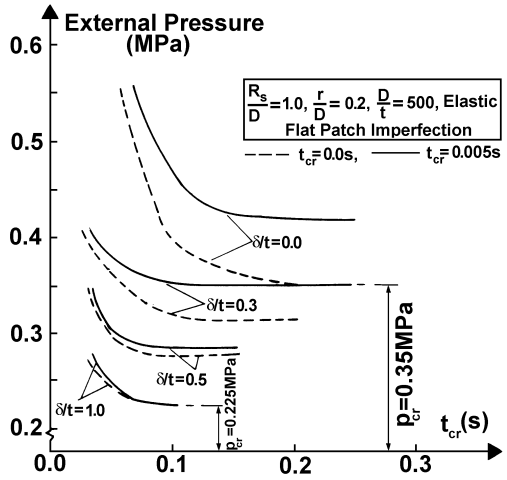

Figure 21. *The effect of the increased-radius flat patch imperfections, δ/t = 0.3, 0.5 and 1.0, on the critical pressure time (for step and ramp pressure profiles)*

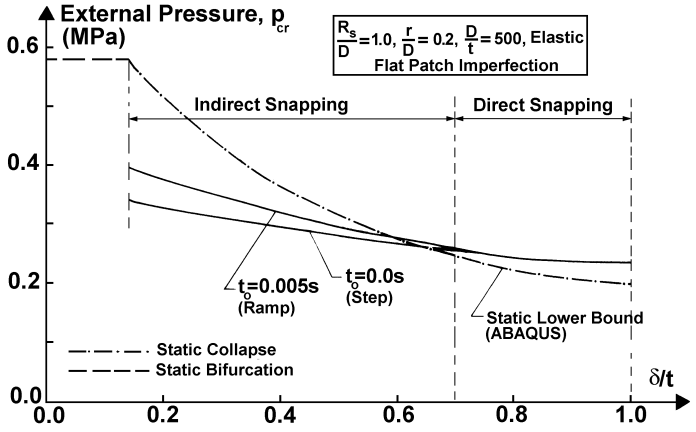

Figure 22. *Comparison of static and dynamic failure loads in geometrically imperfect torisphere*

For ‘larger’ imperfections the situation is reversed - see Figure 22 for a plot of typical results. Table 2 provides comparisons between static and dynamic imperfection sensitivities for a shallow torisphere (with r/D = 0.06).

Table 2. *Comparison of static and dynamic load sensitivities to initial geometric imperfections in the form of an increased-radius flat patch and in the form affine to eigenshape. The elastic response has been recorded for a torispherical head described by $R_s/D = 1.0$, $r/D = 0.06$ and $D/t = 500$. The dynamic load had a step profile (I-S ≡ Indirect Snapping)*

	Flat patch imperfection		Eigenmode imperfection	
δ_o/t	static	dynamic/step	static	dynamic/step
0.0	0.466(12)	0.30(I-S)	0.466(12)	0.30(I-S)
0.25	0.466(12)	--	0.32(6)	0.28(I-S)
0.50	0.312(0)	0.26(I-S)	0.30(6)	0.27(I-S)
0.75	0.243(0)	0.23(I-S)	0.292(6)	0.27(I-S)
1.0	0.196(0)	0.22(I-S)	0.296(6)	0.26(I-S)

7. Summary and conclusions

Computations show that buckling loads for all four shell geometries considered in the paper are sensitive to the initial geometric imperfections. The degree of sensitivity strongly depends on the chosen shape of the imperfection. Other factors include the imperfection’s location and its extent. It has been illustrated by a sample of numerical results that the frequently used imperfection shape in the form affine with the eigenmode corresponding to the lowest eigenvalue can lead, if generalised, to wrong conclusions.

In a cylindrical shell, for example, the eigenmode-type imperfections appear to reduce the load carrying capacity to a much larger extent than localised dimples or narrow stripe-type indents. This may cause unnecessary conservatism in the designs which are based on a knock-down philosophy related to the eigenmode imperfection sensitivity. However one needs to be aware that the latter caters for other uncertainties which are likely to be present in a given component (*e.g.* load application, boundary conditions, etc.). Hence the above observation applies only to situations where influence of other factors is not considered.

The eigenmode shape deviations lead to a smaller buckling load sensitivity in bowed out shells than in mass equivalent cylinders with the corresponding eigen-type imperfections. This demonstrates that ‘optimally’ shaped barrel can be less sensitive to shape imperfections than the equivalent cylinder. This behaviour, however, strongly depends on the geometry of both the cylinder and equivalent bowed out shell. The effect of localised shape deviations on buckling remains to be evaluated.

Studies of toroidal shells with circular cross-sections have shown that eigenvalue-type imperfections do not lead to any appreciable reduction of buckling strength. The situation for elliptical cross-sections becomes more complicated. For some geometries the eigenmode-type imperfections significantly deteriorate the load carrying capacity whilst eigen-imperfections in other geometries do not affect the buckling performance. The localised, inward dimples however can greatly reduce the buckling load across the wide range of semi-axes, (a/b), ratios but only at specific positions on the shell's surface, *e.g.*, at the outer equatorial perimeter. It is clear therefore that assessment of imperfection sensitivity of toroidal shells cannot rely on eigen-type imperfections, only.

The fact that the eigenmode-type shape deviations are not always 'the worst initial shape imperfections' has been illustrated for torispherical shells. The lower bound curve for a localised patch has been obtained numerically and several imperfect configurations were subsequently tested experimentally. It has been found that the imperfection sensitivity manifests itself differently for the spherical portion of the dome and differently for transition region between spherical portion and the knuckle. It is therefore essential to examine both the cap/knuckle junction and the cap itself in order to obtain a safe design.

Comparison between the sensitivity of static and dynamic buckling loads, in an elastic torisphere, reveals that the dynamic loads are more sensitive to eigen-imperfections as well as to the increased-radius flat patches but only for small amplitudes of imperfections. For larger (δ/t)-ratios the opposite situation occurs.

Finally, it is worth noting that all of the above observations are valid for the imperfection amplitude, δ, within the range: $0 \leq \delta/t \leq 1.0$.

8. References

Albertin U., Bemessungskonzepte fuer Stabilitätsfälle imperfektions-sensitiver Schallenstrukturen, PhD Dissertation, TU Munich, 7/2000.

Blachut J., "Pressure vessel components: some recent developments in strength and buckling", *Progress in Structural Engineering and Materials*, Vol. 1, 1998, pp. 415-421.

Blachut J., Jaiswal O.R., "Instabilities in torispheres and toroids under suddenly applied external pressure", *J Impact Engineering*, Vol. 22, 1999, pp. 511-530.

Blachut J., Jaiswal O.R., "On the choice of initial geometric imperfections in externally pressurised shells", *J Pressure Vessel Technology, Trans of the ASME*, Vol. 121, 1999, pp. 71-76.

Blachut J., Jaiswal O.R., "On buckling of toroidal shells under external pressure", *Computers and Structures*, Vol. 77, 2000, pp. 233-251.

Blachut J., Wang P., "Buckling of barreled shells subjected to external hydrostatic pressure", *J Pressure Vessel Technology, Trans of the ASME*, Vol. 123, 2001, pp. 232-239.

Blachut J., "Old and new non-gradient methods in engineering optimization", in *Engineering Methods for Multidisciplinary Optimization*, (eds) J. Blachut, H.A. Eschenauer, CISM Vol. 425, Springer, Wien NY, 2001, pp. 53-105.

Blachut J., "Buckling of externally pressurised barrelled shells: comparison of experiment and theory", *J. Press Vessel Piping*, Vol. 79, 2002, pp. 507-517.

Blachut J., "Optimal barreling of steel shells via simulated annealing", *Computers and Structures*, Vol. 81, 2003, pp. 1941-1956.

Blachut J., "Collapse tests on externally pressurised toroids", *J. Press. Vessel Technology, Trans of the ASME*, Vol. 125, 2003, pp. 91-96.

Brede A., Schneider W., "Imperfection sensitivity of cylindrical shells with longitudinal imperfections subjected to uniform external pressure", in *Design, Inspection, Maintenance and Operation of Cylindrical Steel Tanks And Pipelines*, (ed.) V. Krupka, Brno, 2003, pp. 5-11.

Bushnell D., "BOSOR5 program for buckling of elastic-plastic complex shells of revolution including large deflections and creep", *Computers and Structures*, Vol. 6, 1976, pp. 221-239.

Cederbaum G., Arbocz J., "Reliability of shells via Koiter formula", *Thin-Walled Structures*, Vol. 24, 1996, pp. 173-187.

Galletly G.D., Blachut J., "Stability of complete circular and non-circular toroidal shells", *Proc. IMechE, Part C*, Vol. 209, 1995, pp. 245-255.

Godoy L.A., *Thin-walled structures with structural imperfections*, Elsevier Sci, 1996.

Godoy L.A., Taraco E.O., "Design sensitivity of post-buckling states including material constraints", *Comp. Meth. Appl. Mech. Eng.*, Vol. 188, 2000, pp. 665-679.

Guggenberger W., "Buckling and postbuckling of imperfect cylindrical shells under external pressure", *Thin-Walled Structures*, Vol. 23, 1995, pp. 351-366.

Hallquist J.O., Oasys LS-DYNA940 User's Manual, ver. 7, Livermore Software Co., CA 94550-1740, USA, 1997.

Hibbitt, Karlsson and Sorensen Inc., ABAQUS User's Manual, ver. 5.8, Pawtucket, RI 02860-4847, 1998.

Knight N.F., Jr., Starness J.H., Jr., "Developments in cylindrical shell stability analysis", in Proc. of the *38th AIAA/ASME/ASCE/AHS/ASC Structures, Structural Dynamics and Materials Conference*, Part 3, AIAA-97-1076, 1997, pp. 1933-1948.

Lu Z., Obrecht H., Wunderlich W., "Imperfection sensitivity of elastic and elastic-plastic torispherical pressure vessel heads", *Thin-Walled Structures*, Vol. 23, 1995, pp. 21-39.

Nash W.A., *Hydrostatically loaded structures*, Pergamon, Kidlington, 1995.

Ross C.T.F., *Pressure vessels: external pressure technology*, Horwood Publishing Ltd, Chichester, 2001.

Samuelson L.A., Eggwertz S., *Shell stability handbook*, Elsevier Appl. Sci., London NY, 1992.

Schneider M. H., Jr., “Investigation of the stability of imperfect cylinders using structural models”, *Engineering Structures*, Vol. 18, 1996, pp. 792-800.

Teng J.G, Song C.Y, “Numerical models for nonlinear analysis of elastic shells with eigenmode-affine imperfections”, *Int. J. Solids Struct.*, Vol. 38, 2001, pp. 3263-3280.

Wunderlich W., Albertin U., “Buckling of imperfect spherical shells”, *Int. J. of Non-Linear Mech.*, Vol. 37, 2002, pp. 589-604.